Phonon-assisted exciton relaxation dynamics for a (6,5)-enriched DNA-wrapped single-walled carbon nanotube sample

S. G. Chou,[1] M. F. DeCamp,[1] J. Jiang,[2] Ge. G. Samsonidze,[3] E. B. Barros,[3,4] F. Plentz,[5] A. Jorio,[5] M. Zheng,[6] G. B. Onoa,[6] E. D. Semke,[6] A. Tokmakoff,[1] R. Saito,[2] G. Dresselhaus,[7] and M. S. Dresselhaus[3,8]

[1]*Department of Chemistry, Massachusetts Institute of Technology, Cambridge, Massachusetts 02139-4307, USA*

[2]*Department of Physics, Tohoku University and CREST JST, Aoba, Sendai 980-8578, Japan*

[3]*Department of Electrical Engineering and Computer Science, Massachusetts Institute of Technology, Cambridge, Massachusetts 02139-4307, USA*

[4]*Departamento de Física, Universidade Federal do Ceará, Fortaleza-CE, 60455-760, Brazil*

[5]*Departado de Física, Universidade Federal de Minas Gerais, Belo Horizonte-MG, 30123-970, Brazil*

[6]*DuPont Central Research and Development, Experimental Station, Wilmington, Delaware 19880-0328, USA*

[7]*Francis Bitter Magnet Laboratory, Massachusetts Institute of Technology, Cambridge, Massachusetts 02139-4307, USA*

[8]*Department of Physics, Massachusetts Institute of Technology, Cambridge, Massachusetts 02139-4307, USA*

(Received 18 June 2005; published 15 November 2005)

A series of nondegenerate pump-probe measurements were carried out on a DNA-wrapped single-walled carbon nanotube (SWNT) sample that is enriched with the (6,5) species. The pump pulse excites SWNTs at ~1.567 eV, which corresponds to an energy of two *D*-band phonons above the excitonic band edge of the (6,5) SWNT. The dynamics of different channels of exciton relaxation for the (6,5) SWNT is analyzed in terms of the decay in the time-resolved differential transmission spectra. By systematically varying the values of the probe energy, E_{probe}, to be in and out of resonance with the minority (n,m) SWNT species in the sample at different pump fluence levels, an intermediate decay component associated with a hot phonon-absorption process is studied in detail. When the values of E_{probe} were further tuned to off-resonance positions, photoinduced absorption processes could be investigated.

DOI: 10.1103/PhysRevB.72.195415 PACS number(s): 78.30.Na, 78.30.−j, 78.66.Tr

I. INTRODUCTION

Understanding the different channels of relaxation for optically excited electrons in one-dimensional systems has played a crucial role in developing potential applications for optoelectronic devices in nanoscale systems. As a prototype one-dimensional (1D) material, single-walled carbon nanotubes (SWNTs) and their optical properties have been a subject of intense study.

Numerous time-resolved, pump-probe studies of individually dispersed SWNTs have provided important information for understanding the dominant excitonic relaxation channels,[1–8] yet the detailed mechanisms of many subtler relaxation processes remain less understood. In most prior studies, the relaxation dynamics for optically excited SWNTs has often been found to be dominated by a single exponential or biexponential decay, consisting of a fast, subpicosecond decay associated with intraband relaxation processes, followed by a slow, 10–180 ps process associated with a resonantly enhanced recombination process originating from the excitonic band edge.[3–10] On some occasions, an intermediate decay time of 2–5 ps can be observed in nondegenerate pump-probe studies when the pump energy, E_{pump}, is offset from the probe energy, E_{probe}, by an energy of two or more optical phonons.[11] Preliminary explanations have been suggested to account for this observation,[11] but no systematic study has yet been carried out to understand such a process in detail.

To further understand this intermediate decay process, a series of pump-probe measurements were carried out on a (6,5) enriched SWNT sample, in which the SWNTs are partially wrapped with single-stranded DNA. Since two phonon assisted absorption and relaxation processes have been found to be prominent excitonic processes in DNA-wrapped SWNTs,[12] the value of the E_{pump} was selected to be very close to $E_{11}^{1A-}(6,5)+2\hbar\omega_D$, where $2\hbar\omega_D$ corresponds to the energy for two *D*-band phonons and $E_{11}^{1A-}(6,5)$ denotes the energy for the band-edge excitonic state with orbital symmetry $1A-$ (also called the $1s$ excitonic state[13,14]). The pump excitation was especially chosen to enhance the electron-phonon coupling and double resonance process associated with *D*-band phonons.[15]

The optical response is measured in terms of the differential transmission (DT) of the probe beam, $\Delta T/T_o$, which corresponds to the fractional difference in transmission intensity between the pump-induced transmission, T, and the transmission of the reference beam (with no pump influence), T_o, where $\Delta T=T-T_o$. The DT intensity is negative for photoinduced absorption and is positive for photobleaching. From the exponential decay of the DT spectra, multiple processes associated with different decay time scales can be resolved.[16]

With a (6,5) enriched sample[17] and a carefully selected energy for E_{pump}, we examine the physical process governing this well-resolved intermediate decay component in detail. By systematically varying the values of E_{probe} to be in and out of resonance with the majority (6,5) and minority (n,m) SWNT species in the sample at different pump fluence levels, we were able to link the intermediate decay time component associated with the (6,5) SWNT directly to the depletion of the band-edge exciton population caused by hot

phonon absorption. Photoinduced absorption processes were also observed when the selected values of E_{probe} correspond to off-resonance energies. When taken together, these time-resolved experiments clarify the role of both hot phonon-assisted band-edge exciton depletion processes and the Auger process in the relaxation of excitons for individual SWNTs.

II. EXPERIMENTAL

To obtain detailed information about phonon-mediated PL processes, it is highly desirable to have one dominant (n,m) species in the sample. The DNA-wrapped sample was prepared from SWNTs produced by the CoMoCAT process.[18] From the CoMoCAT-based, DNA-wrapped starting material, the (6,5) enriched sample was then prepared using ion exchange chromatography,[17] and the pump-probe measurements were made in a 400 μL glass spectrophotometer cell with a 1 mm optical path.

A two-color pump-probe system was used for the pump-probe measurements. The probe pulse was generated by a home-built optical parametric amplifier (OPA), which was pumped by a 1.567 eV, 1 kHz laser system. The OPA was tuned from 1.272 to 1.158 eV to produce different values of E_{probe}. The transmitted probe pulse was collected by a fast silicon photodiode. The pump pulse intensity was controlled by a waveplate-polarizer pair. The pump pulse was chopped at 500 Hz, and a lock-in amplifier collected the modulated probe signal. The temporal and spatial cross-correlation of the pump and the probe pulses gives an instrument resolution of ~250 fs. The relative timing between the pump and probe pulses was maintained by a computer-controlled mechanical delay line.

III. RESULTS

Figure 1 shows a typical differential transmission (DT) spectrum as a function of the pump-probe delay time. The $E_{\text{pump}} \sim 1.567$ eV was close to the energy of $E_{11}^{1A^-}(6,5) + 2\hbar\omega_D$, while E_{probe} was set at ~1.252 eV, which is close to the previously determined $E_{11}^{1A^-}(6,5)$ band edge for DNA-wrapped SWNTs.[12,19] The $2\hbar\omega_D$ here denotes the energy of two D-band phonons for SWNTs.

The decay in the DT intensity, $I(t)$, as a function of delay time, t, can be decomposed into a simple multiexponential decay function

$$I(t) = \sum_{i}^{j} A_i e^{-t/\tau_i} \tag{1}$$

in which the coefficient A_i denotes the relative weight of the ith process associated with decay time τ_i. For the present experiment, a triexponential ($j=3$) decay function can be resolved.

Upon excitation from the pump pulse, numerous excitons are created at an exciton-bound phonon state corresponding to E_{pump}, from which most of the excitons nonradiatively decay to the band edge $E_{11}^{1A^-}(6,5)$, forming a very fast rise (<200 fs) in the DT intensity due to the dominant (6,5) SWNT. This filling of the band-edge exciton state is followed by a triexponential decay process, as shown in Fig. 1. The spectral decomposition of the spectrum in Fig. 1 shows that the initial 20 ps of the decay is dominated by two exponential decay terms in Eq. (1), each associated with a decay time of ~700 fs(±10%) and ~2–3 ps(±10%), respectively, and the two decay terms each account for ~45% of the initial 20 ps of the decay process. In addition, a small amount of the exciton decay process is associated with a slow process with a much longer decay time.

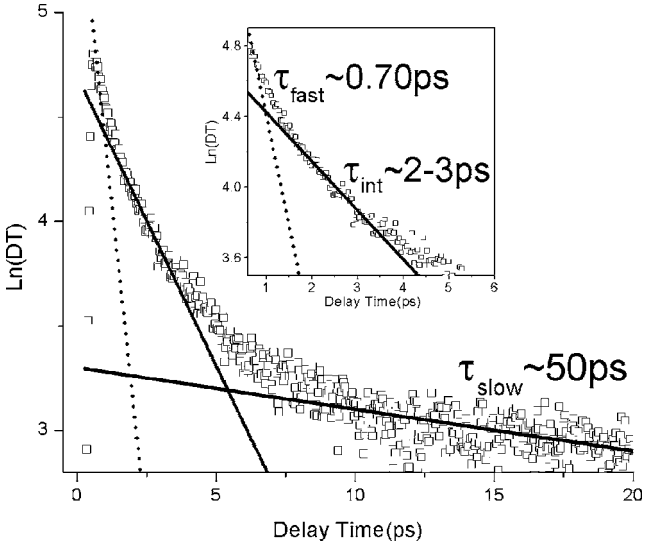

FIG. 1. A transient spectrum monitoring the DT intensity vs delay time, for $E_{\text{probe}} \sim E_{11}^{1A^-}(6,5)$ at 1.252 eV, for a (6,5) enriched DNA-wrapped nanotube sample, pumped with $E_{\text{pump}} \sim 1.567$eV (pump fluence level fixed at 0.1 J/m^2). The $\Delta T/T_o$ data are plotted on a natural log scale. The inset shows a magnified portion of the plot to show the range of the delay time, pertinent to τ_{int} more clearly.

To gain physical insights into the decay processes, the pump fluence dependence of the individual processes (τ_{fast}, τ_{int}, and τ_{slow}) was studied by keeping E_{probe} close to $E_{11}^{1A^-}(6,5)$. Figures 2(a) and 2(b) show the decay time evolution for the three processes identified in Fig. 1 at different pump fluence.[20] Both τ_{slow} and τ_{int} show a clear pump fluence dependence, in which the decay processes occur faster with increasing fluence, whereas the fluence dependence for τ_{fast} is less clear within the range of available pump fluence levels.

Figure 2(c) shows the relative weights in Eq. (1) for each of the three components during the initial 20 ps decay at different levels of pump fluence. The relative weight for τ_{int} is found to increase with pump fluence. As discussed in the next section, the result of the increased weight of τ_{int} with increasing pump fluence substantiates the proposed interpretation accounting for the intermediate decay time component, which involves an additional channel of phonon-mediated excitonic relaxation.

In order to further establish the identifications for the various decay processes, we extend the two-color experiment to excite different (n,m) SWNTs for which the E_{pump} does not correspond to specific exciton-phonon states.[12] We scrutinize

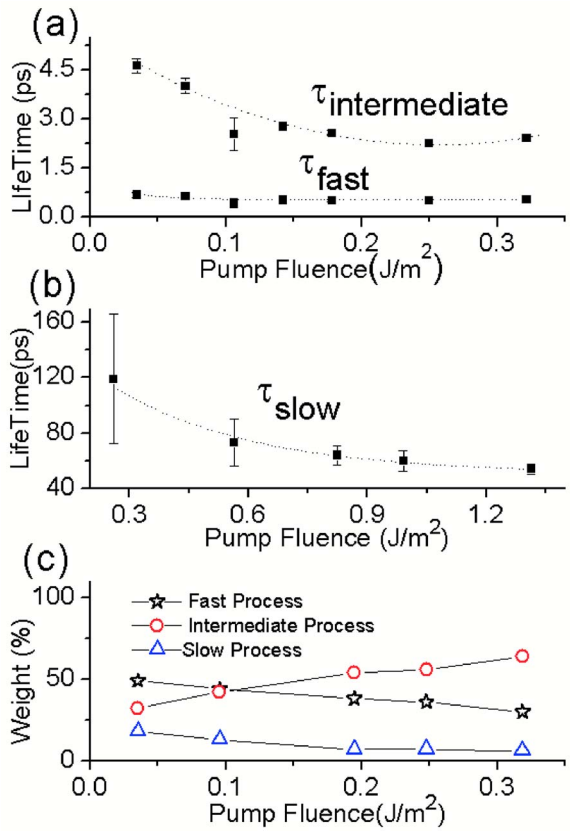

FIG. 2. (Color online) Fluence dependence of the different components in the relaxation dynamics for $E_{probe} \sim 1.252$ eV. The dotted lines are guides to the eyes. The faster components were measured with higher time resolution (40 fs), over 20 ps. To determine τ_{slow} more accurately, fluence-dependent experiments were carried out over 50 ps with lower time resolution (120 fs) and higher pump fluence. Fluence dependence of (a) the two faster components corresponding to intraband processes and (b) the slower component corresponding to the dynamics of the interband recombination. (c) Shows that for the initial 20 ps of the decay process, the relative weight for the intermediate process increases with the pump fluence.

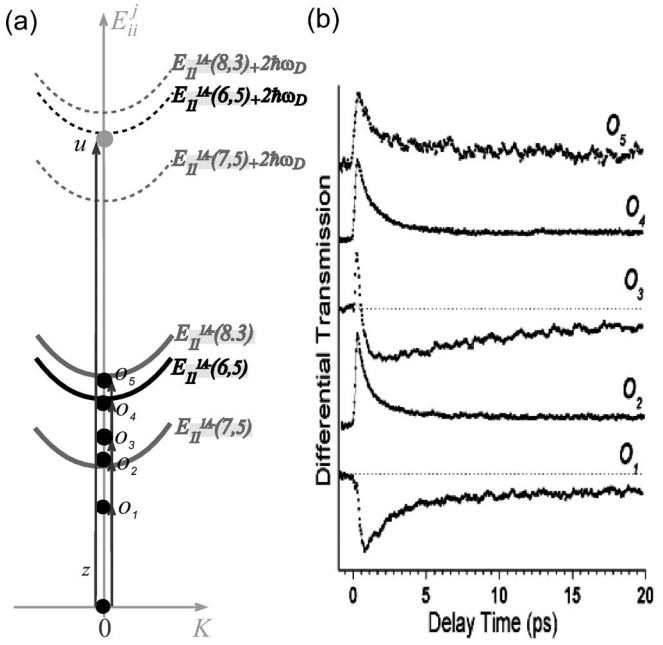

FIG. 3. The schematic diagram and the respective DT spectra for five different probe energies. (a) A schematic diagram of different values of E_{probe} relative to the band-edge energies of different nanotubes. The values of E_{probe} from O_1 to O_5, respectively, are 1.158, 1.198, 1.222, 1.252, and 1.272 eV. (b) DT spectra for different values of E_{probe}. Notice that DT changes sign as E_{probe} moves in and out of resonance with the (6,5) and (7,5) nanotubes. We use the dotted lines as guides for the eyes to mark the zero DT line for the respective DT spectra. The positive DT intensities are normalized to aid with the line-shape comparison.

the relaxation dynamics more generally by monitoring the DT spectral profiles when tuning E_{probe} between 1.158 and 1.272 eV at four values of E_{probe} that are different from $E_{probe}=E_{11}^{1A-}(6,5)$. The positions of the different E_{probe}, relative to the band-edge energies of different (n,m) species in the sample, correspond to O_1, O_2, O_3, and O_5 in the schematic band diagram shown in Fig. 3(a).

In the cases of O_2 and O_5 in Fig. 3(a), the values of E_{probe} are close to the band-edge energies, $E_{11}^{1A-}(7,5)$ and $E_{11}^{1A-}(8,3)$, for two minority species in the sample. In these cases, even though a photobleaching behavior is also observed, the relative weight distributions for the individual decay processes are quite different from the case when $E_{probe} \sim E_{11}^{1A-}(6,5)$ is in resonance with the majority (6,5) SWNTs in the sample. Lower overall signal intensities were obtained for the minority (7,5) and (8,3) SWNTs. Also, when the values of E_{probe} are chosen such that E_{probe} no longer corresponds to any band-edge energy, as shown in Fig. 3(a) by traces O_1 and O_3 , the intensity of the DT spectrum drops to negative values before rising back to equilibrium with time evolution, as shown in the DT spectra corresponding to O_1 and O_3 in Fig. 3(b). The negative DT intensity suggests the presence of a photoinduced absorption process. The analysis of the two different rising components, as will be discussed later, indicates that the different rise components in O_1 and O_3 mirror the decay times of the (6,5) SWNTs shown in Fig. 1, but include contributions from all (n,m) species in the sample.

IV. DISCUSSION

A. State filling via exciton-phonon interactions

In general, we determine the relative exciton population at the state being probed by E_{probe} from the corresponding DT intensity profile. The rising segment in a DT spectrum corresponds to state-filling processes and the decaying segments correspond to population depletion processes at an energy corresponding to E_{probe}.

Because of the enhanced population of (6,5) SWNTs and the corresponding reduced interference from optical signals originating from the other (n,m) SWNTs in the sample, we first set the E_{pump} at $E_{11}^{1A-}(6,5)+2\hbar\omega_D$ and E_{probe} at the $E_{11}^{1A-}(6,5)$ band edge to study the pump-induced excitonic filling and depletion of the $E_{11}^{1A-}(6,5)$ band edge.

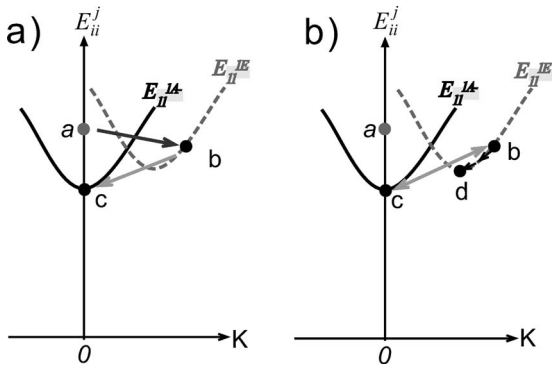

FIG. 4. (a) A schematic diagram of relaxation from a to the $1A-$ excitonic state c by emitting two D-band phonons (see text). The black arrow denotes a fast phonon-emission process originating from an exciton-bound phonon state, whereas the gray arrow denotes a slow process originating from a real excitonic state. (b) A schematic diagram of a scenario in which the band-edge exciton population can be depleted via phonon absorption. The experiment was carried out for the case where $E_{\text{probe}}=E_{11}^{1A-}(6,5)$, corresponding to point c.

As shown in Fig. 1, upon excitation by the pump pulse, a sharp initial rise was observed within the first 200 fs [see Fig. 3(a), trace O_4]. This sharp rise can be related to rapid state-filling processes at the $E_{11}^{1A-}(6,5)$ band edge. In most two-color pump-probe studies where $E_{\text{pump}}\sim E_{11}^{1A-}(n,m)+\Delta E$ and $E_{\text{probe}}\sim E_{11}^{1A-}(n,m)$, the (n,m) band-edge state is filled by the E_{pump}-created higher-energy excitons which lose energy via phonon-emission events involving many different phonons.[6] In the present study, the excitons created by E_{pump} have an energy such that the energy difference between the pump and the probe pulses corresponds to the energy of two D-band phonons. As a result, a special band-edge filling process occurs, and a large fraction of the excitons created at 1.567 eV is expected to efficiently relax nonradiatively to fill the $E_{11}^{1A-}(6,5)$ band edge, following the mechanism described in Fig. 4(a) and discussed below.

Upon pump excitation, a large number of excitons are created by the pump pulse at state a in Fig. 4(a), from which the exciton can quickly emit a D-band phonon with momentum q to access a dark exciton state with E symmetry,[21,22] denoted by b in Fig. 4(a). From b, which is a real excitonic state, a second D-band phonon with momentum $-q$ can be emitted to bring the exciton to the $E_{11}^{1A-}(6,5)$ band-edge state c. The mechanisms of the phonon scattering processes are specified by the symmetry of the phonon and the excitonic states.[23] In general, in carbon nanotubes, the A-symmetry Γ-point phonons such as radial breathing modes and G-band phonons, and the E-symmetry K point zone boundary D-band phonons are the specific phonons that participate frequently in such scattering events. An A-symmetry Γ-point phonon would scatter an A-symmetry exciton to another A-symmetry excitonic state and an E-symmetry exciton to another E-symmetry excitonic state.[23] Similarly, an E-symmetry phonon would scatter an A-symmetry exciton to an E-symmetry excitonic state and vice versa.[23] Since the D-mode process is strong for E-symmetry phonons associated with electron-phonon coupling near the K point of the Brillouin zone,[24] scattering events involving a D-band phonon will couple an A-symmetry zone-center exciton band-edge state to an E-symmetry dark exciton state.

Because of the high efficiency for the two optical-phonon scattering processes described above [in Fig. 4(a)], we expect this mechanism to contribute significantly to the initial rise in the $E_{11}^{1A-}(6,5)$ band-edge exciton population, and a large number of D-band phonons will thus be created. Such hot phonons exist as quantized lattice vibrations associated with individual SWNTs in addition to the ordinary phonon distribution expected at a given temperature. Therefore, we use the term "hot" phonons to describe these nonequilibrium D-band phonons. These lattice vibrations can be transferred from one SWNT to a neighboring SWNT in solution via collisions.

Even though the energy chosen for E_{pump} in this experiment is close to the position of the previously reported $E_{11}^{2A+}(6,5)$ (or $2p$ exciton) level[13,14] for (6,5) SWNTs, we do not populate the $E_{11}^{2A+}(6,5)$ level significantly by the intense pump pulse because the optical symmetry selection rule dictates that such a state cannot be accessed with a one-photon excitation process.[13,14] Thus, the resulting pump-induced decay dynamics should not be much affected by the $E_{11}^{2A+}(6,5)$ state.

B. Different decay channels

After the rapid initial state filling process is completed within the first 200 fs, the DT spectra in Fig. 1 show three different components of exponential decay that correspond to three channels of band-edge exciton depletion, with decay times τ_{fast}, τ_{int}, and τ_{slow}. The fast and the slow processes have been described and studied in detail in previous studies,[1,2,10] while the detailed mechanism of the intermediate process has not yet been clarified.

The fast, subpicosecond decay term observed in Fig. 1 has long been correlated with band-edge decay processes that are electronic in origin.[7,10,25,26] Even though multiple mechanisms have been suggested to account for this process,[7,25,26] prior pump-probe studies have shown that such a fast initial decay process is usually dominated by Auger processes,[4,25] whereby the collision of two excitons results in the annihilation of one of the excitons, which nonradiatively recombines. The excess of energy from the recombination event is transferred to the other participating exciton, resulting in either the dissociation of that exciton into a free electron and hole in the continuum, or the promotion of the exciton into $E_{22}^{1A-}(6,5)$, as described in Ma *et al.*[4] The free electron and hole in the continuum will further recombine via multiple recombination pathways without contributing to the DT spectra observed at E_{probe}.

The slow decay component has a decay time scale, $\tau_{\text{slow}}\sim 50$ ps, and this range of long decay times is consistent with previously identified long decay time mechanisms.[7] Since the quantum yield for the radiative recombination process for SWNTs is low (10^{-4}),[27] a large fraction of the recombination events are expected to occur nonradiatively. Thus, we assign the slow decay component to contain contributions from both a weak radiative recombination process and a dominant

TABLE I. Decay times and weights of the individual processes measured at different probe energies.

E_{probe}	Pump fluence (J/m^2)	τ_{fast} (fs)	A_{fast} (%)	τ_{int} (ps)	A_{int} (%)	τ_{slow} (ps)	A_{slow} (%)
1.272 eV	0.3	~900	~70	several ps traces mixed with τ_{slow}		~30	~30
1.252 eV	0.1	~700	~45	3.0	~45	~50	~10
1.198 eV	0.3	~800	~90	N/A	N/A	~40	~10

phonon-assisted relaxation process, in which the band-edge excitons are slowly depleted via phonon scattering. One such possible nonradiative decay scenario shows the decay of the E_{11}^{1A-} band-edge excitons via exciton-phonon interactions which slowly decay into defect-induced trap states below the $E_{11}^{1A-}(6,5)$ band edge.[23]

The intermediate decay process is a more subtle process that only appears under special circumstances when the energy difference between the pump and the probe pulses corresponds to two or more phonon energies, and where the phonon in question is associated with a highly efficient phonon-assisted process. The specificity observed in this study suggests that the τ_{int} decay process can be attributed to the depletion of the band-edge exciton population via the absorption of a specific phonon by the (6,5) SWNT. In general, one expects such a phonon-absorption process to be in equilibrium with the corresponding phonon-emission events. Such a process would keep the band-edge population at a steady state. However, it is possible, after a phonon-absorption event, that the exciton in question relaxes via other channels without returning to the band edge, resulting in a net decrease in the $E_{11}^{1A-}(6,5)$ band-edge exciton population. One such scenario is described in Fig. 4(b).

As described earlier, during the initial exciton population buildup, a large number of hot D-band phonons are created by two phonon emission processes $a \rightarrow b$ and $b \rightarrow c$, as shown in Fig. 4(a). Given the large abundance of hot D-band phonons for the first ps after the onset of the pump pulse, it is possible for the exciton at the band edge c to absorb a D-band phonon and return to b, thus establishing a quasi-equilibrium $c \rightleftharpoons b$, as shown in Fig. 4(b). However, a small fraction of the excitons at b, instead of following the $b \rightarrow c$ path and returning to the $E_{11}^{1A-}(6,5)$ band edge, can scatter with one or more small energy phonons and can leak into the band edge of the dark exciton state d. As shown in Fig. 4(b), once the exciton at b relaxes to d, the exciton will likely be trapped and never return to c. Under this scenario, the "leaking" process will drive the equilibrium $c \rightleftharpoons b$ to the right and remove excitons from $E_{11}^{1A-}(6,5)$ permanently at the rate of the leaking process. Under this scenario, the τ_{int} reflects the rate at which the exciton at b leaks into d.

With the above described relaxation channels in mind, we can now understand the effects observed with increasing pump fluence. With increasing pump fluence, more excitons can be created at 1.567 eV, and these excitons subsequently decay via hot phonon generation. As a result, the rate of hot D-band phonon generation increases with pump fluence, which increases the relative rate of exciton depletion at the $E_{11}^{1A-}(6,5)$ band edge via the phonon absorption process described above and in Fig. 4(b). This mechanism is consistent with the observed pump fluence dependence for τ_{int}. On the other hand, with increasing fluence, even though more excitons are being generated at the $E_{11}^{1A-}(6,5)$ band edge and the rate of the electronic relaxation channel (such as Auger process) is more sensitive to the band-edge exciton population, little fluence dependence is expected for τ_{fast}. Our data show a possible small fluence dependence for τ_{fast} at low fluence levels in Fig. 2(a), but the relative weight of τ_{fast} decreases with increasing fluence. However, the detailed fluence dependence is not well resolved, in our data, for such a short decay time.

In general, we would expect a similar phonon-mediated state filling process and depletion process to be present for all (n,m) species, provided that $E_{pump} \sim E_{11}^{1A-}(n,m) + 2\hbar\omega_D$ for the particular (n,m) SWNT. However, out of the few prior pump-probe studies that have met these special energy requirements,[11] the measurements were carried out on samples with many (n,m) species. For such samples, only a small percentage of the SWNTs in the sample could experience the special hot phonon process observed here for the (6,5) SWNT and therefore the observed effects were smaller in magnitude than what is seen in our study.

In the present study, the hot phonon processes become a very pronounced feature in the resulting DT spectra for a (6,5) enriched SWNT sample. The increasing importance of the τ_{int} process with increasing fluence shown in Fig. 2(c) substantiates the phonon-assisted nature of this process. Note that Fig. 2(c) shows the relative weights of the three processes within the first 20 ps. Even though the fast Auger process might be speeding up with increasing fluence, its relative weight appears to be decreasing while the weight of the clearly resolved intermediate process is increasing faster.

C. Probing the minority species in the sample

The energy specificity for the hot phonon creation and absorption processes that lead to filling and depletion of the band-dge exciton population can be demonstrated by the measurements carried out when E_{probe} is tuned to the E_{11}^{1A-} band edge of the minority species in the sample, as represented by transitions O_2 and O_5 in the schematic energy level diagram shown in Fig. 3(a).

For O_2 and O_5 in Fig. 3(a), the values of E_{probe} are close to the $E_{11}^{1A-}(7,5)$ and $E_{11}^{1A-}(8,3)$ band-dge states, respectively. As mentioned before, even though similar positive spectral profiles as Fig. 1 are observed, the different relative weight distributions for the individual decay processes suggest a difference in the intrinsic decay mechanisms involved.

Table I shows the normalized weights of the different processes in the DT spectra measured with different values of E_{probe}. With $E_{11}^{1A-}(6,5) + 2\hbar\omega_D$, three separate components can be resolved, as described in Fig. 1. When E_{probe} is close

to $E_{11}^{1A^-}(7,5)$ [trace O_2 in Fig. 3(b)], a biexponential decay dynamics is observed, and the decay time scales for the two components are consistent with previous pump-probe studies.[1–10] E_{pump} (1.567 eV) here still corresponds to $E_{11}^{1A^-}(7,5)+\Delta E$, but ΔE no longer corresponds to $2\hbar\omega_D$. Thus for the (7,5) SWNT, the DT decay does not get a significant contribution from the hot *D*-band phonon absorption process. The absence of the intermediate decay time component in this case supports the aforementioned identification that correlates τ_{int} with the depopulation of $E_{11}^{1A^-}$ band-edge states via hot *D*-band phonon-absorption processes.

When E_{probe} was tuned to ~1.272 eV [trace O_5 in Fig. 3(b)], which is close to $E_{11}^{1A^-}(8,3)$, it is possible to decompose the exponential decay into three components, but the intermediate component is not clearly resolved. If instead the transient spectrum is characterized by a biexponential decay, we find that both τ_{slow} and τ_{fast} are shifted slightly compared to the values obtained from the (6,5) and (7,5) SWNTs using three exponentials in the fit. Since the value of $E_{11}^{1A^-}(8,3)+2\hbar\omega_D$ is ~34 meV higher than $E_{\text{pump}}=1.56$ eV, it is possible for the tail of the E_{pump} to access $E_{11}^{1A^-}(8,3)+2\hbar\omega_D$ and trigger similar filling and depletion processes for the $E_{11}^{1A^-}(8,3)$ band-edge exciton population by the hot phonon generation and absorption process described above. These hot phonons can thus contribute weakly to the DT decay and give rise to a small τ_{int} component. As a result, τ_{int} can then contribute weakly to the DT decay and can get partially mixed with τ_{fast} and τ_{slow}. The unresolved τ_{int} component makes τ_{fast} a little longer and τ_{slow} a little shorter. Since the $E_{11}^{1A^-}(8,3)$ energy is very close to that for $E_{11}^{1A^-}(6,5)$, and since the (8,3) SWNT is a minority species in the sample, it is possible that we are also observing optical responses from some (6,5) SWNTs in the sample. A sample strongly enriched in (8,3) nanotubes will be needed to distinguish the different contributions to the relaxation process more clearly.

The detailed similarities and differences of the relaxation processes for the (6,5), (7,5), and (8,3) SWNTs thus provide a better understanding of the relaxation process for the (6,5) SWNTs. Since the (7,5) and (8,3) SWNTs are minority species in the sample, the pump-probe signals corresponding to these tubes are weaker than the signal correlated with the (6,5) SWNTs, and, therefore, a higher pump fluence has to be used to induce a noticeable optical response. Even though the experiments are carried out here under different pump fluence conditions, it is still possible to qualitatively compare the overall weights of the intermediate decay components for these different SWNTs and to reach some conclusions about the physical mechanisms that are involved.

D. Photoinduced absorption processes

The negative DT intensities for the cases of O_1 and O_3 in Fig. 3(b) suggest the presence of photoinduced absorption processes. Similar absorption processes have been observed in prior pump-probe studies,[1,6,28–30] under different experimental conditions, and multiple physical models have been proposed to account for these observations.[1,2,6,28]

In the present experiment, since the values of E_{probe} remain in the IR range, it is not likely that the observed photo-

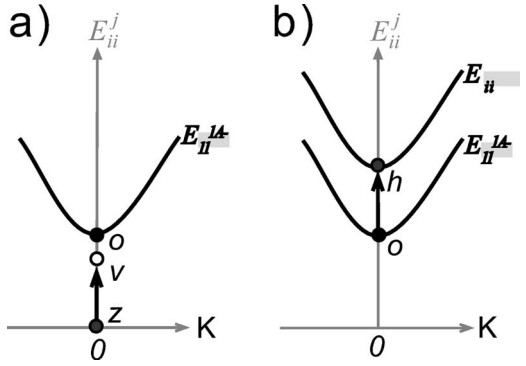

FIG. 5. Schematic diagram of two possible scenarios for the photoinduced absorption process when E_{probe} does not correspond to excitonic band-edge energies. (a) A band-edge exciton at *o* is created by exciting an electron from ground state *z* to virtual state *v* and combining with an optical phonon. (b) A band-edge exciton at *o* can combine with a photon and access a higher continuum mobile band state at E_{ii}, denoted by *h*.

induced absorption is introduced by plasmon interactions as described in a previous report.[29] As shown in Fig. 3, the values of E_{probe} at O_1 and O_3 do not have the right energies for exciton creation for the SWNTs contained in our sample, as shown in Fig. 5(a) for *z* to *v*. The photons from the E_{probe} pulse in this case can in fact be absorbed by the $E_{11}^{1A^-}$ band-edge excitons at *o* (which had been previously created by the pump pulse) by promoting these band-edge excitons into either another higher band-edge state or to a continuum mobile band state, denoted by $E_{ii}^{1A^-}$ in Fig. 5(b). The pump-induced absorption events will decrease the corresponding optical transmission at the corresponding E_{probe} and will result in negative DT intensities. Under this model, the probe beam probes the population of the band-edge states of the SWNTs in the sample indirectly through photoinduced absorption, and the time scale for the exponential rise should closely mirror the time scale for the exponential decay in the cases of photobleaching, when a specific band-edge state is being probed. A detailed description of such photoinduced absorption processes is described in Korovyanko *et al.*[1] According to this model,[1] the photon energy of the E_{probe} is absorbed by a band-edge exciton with no physical mechanism to discriminate one (n,m) SWNT from another. As a result, all of the (n,m) species in the sample should contribute to the photoinduced absorption process. However, since our sample is enriched in (6,5) SWNTs, the DT spectra should mostly mirror the changes in the $E_{11}^{1A^-}(6,5)$ band- edge population with time evolution.

For the cases of O_1 and O_3 in Fig. 3(b), the rising part of the spectra can be decomposed into multiple components using an expression similar to Eq. (1),

$$I(t)=\sum_{i}^{j} A_i(1-e^{-t/\tau_i}). \tag{2}$$

Spectral analysis shows that the observed exponential rise in O_1 and O_3 can both be fit with a biexponential function with two ranges of rise time: $\tau_{\text{rise1}}\sim 1-9$ ps and τ_{rise2}

$\sim 30-100$ ps. The two ranges of rise times in the photoinduced absorption spectra are qualitatively consistent with the ranges of τ_{int} and τ_{slow}, observed in the cases when $E_{\text{probe}} \sim E_{11}^{1A^-}(6,5)$ and where photobleaching occurs. The experimental observations in Fig. 3(b) substantiate the model proposed above.

In the case of $E_{\text{probe}} \sim 1.222$ eV, shown as O_3 in Fig. 3, the DT spectrum also shows a small positive peak before the intensity drops below zero. The small positive DT peak is attributed to the tail of the broad probe beam that excites excitons directly into the $E_{11}^{1A^-}(7,5)$ band-edge state at 1.19 eV, which is ~ 30 meV from the E_{probe} centered energy, resulting in a small amount of photobleaching for short times after the pump is fired.

V. SUMMARY

In this study, by using a carefully chosen E_{pump} that corresponds to $E_{11}^{1A^-}(6,5)+2\hbar\omega_D$ and probing at $E_{11}^{1A^-}(6,5)$, an intermediate decay time component that is associated with the hot D-band phonon-absorption relaxation process is studied in detail. By systematically varying the pump fluence and by varying the values of E_{probe} to be in and out of resonance with the minority (n,m) SWNT species in the sample, we looked into the detailed similarities and differences in the different channels of band-edge exciton population decay mechanisms for the (6,5), (7,5), and (8,3) SWNTs. The detailed information thus obtained from the experiment clarifies the role of hot phonon absorption and emission processes, as well as the Auger process, in the filling and depletion of band-edge exciton populations for individual SWNTs.

ACKNOWLEDGMENTS

The MIT authors acknowledge support under Dupont-MIT Alliance, NSF Grants No. DMR 04-05538, No. INT 00-00408, and DOE Grant No. DEFG02-99ER14988. S.G.C. thanks Professor R. B. Capaz for stimulating discussions, clarifying different aspects of dark exciton states. The Brazilian authors acknowledge support from the Instituto de Nanosciencias, Brazil. E.B.B. acknowledges support from CAPES-Brazil. R.S. acknowledges a Grant-in-Aid (No. 16076201) from the Ministry of Education, Japan.

[1] O. J. Korovyanko, C.-X. Sheng, Z. V. Vardeny, A. B. Dalton, and R. H. Baughman, Phys. Rev. Lett. **92**, 017403 (2004).

[2] J. S. Lauret, C. Voisin, G. Cassabois, C. Delalande, Ph. Roussignol, O. Jost, and L. Capes, Phys. Rev. Lett. **90**, 057404 (2003).

[3] Y. Z. Ma, J. Stenger, J. Zimmermann, S. M. Bachilo, R. E. Smalley, R. B. Weisman, and G. R. Fleming, J. Chem. Phys. **120**, 3368 (2004).

[4] Y. Z. Ma, L. Valkunas, S. L. Dexheimer, S. M. Bachilo, and G. R. Fleming, Phys. Rev. Lett. **94**, 157402 (2005).

[5] G. N. Ostojic, S. Zaric, J. Kono, M. S. Strano, V. C. Moore, R. H. Hauge, and R. E. Smalley, Phys. Rev. Lett. **92**, 117402 (2004).

[6] G. N. Ostojic, S. Zaric, J. Kono, V. C. Moore, R. H. Hauge, and R. E. Smalley, Phys. Rev. Lett. **94**, 097401 (2005).

[7] J. Kono, G. N. Ostojic, S. Zaric, M. S. Strano, V. C. Moore, J. Shaver, R. H. Hauge, and R. E. Smalley, Appl. Phys. A: Mater. Sci. Process. **78**, 1093 (2004).

[8] D. J. Styers, S. P. Ellison, C. Park, K. E. Wise, and J. M. Papanikolas, J. Phys. Chem. A **109**, 289 (2005).

[9] A. Hagen and T. Hertel, Nano Lett. **3**, 383 (2003).

[10] A. Hagen, G. Moos, V. Talalaev, and T. Hertel, Appl. Phys. A: Mater. Sci. Process. **78**, 1137 (2004).

[11] I. V. Rubtsov, R. M. Russo, T. Albers, P. Deria1, D. E. Luzzi, and M. J. Therien, Appl. Phys. A: Mater. Sci. Process. **79**, 1747 (2005).

[12] S. G. Chou, F. Plentz, J. Jiang, R. Saito, D. Nezich, H. B. Ribeiro, A. Jorio, M. A. Pimenta, G. G. Samsonidze, A. P. Santos, M. Zheng, G. B. Onoa, E. D. Semke, G. Dresselhaus, and M. S. Dresselhaus, Phys. Rev. Lett. **94**, 127402 (2005).

[13] The total parity of the exciton is given by a product of translational σ_n and circumferential parity σ_X: $\sigma_{\text{total}}=\sigma_n \otimes \sigma_X$. In the translational direction, the envelope function in the 1D H atom model is either symmetric (0 nodes, $n=1$) or antisymmetric (1 node, $n=2$). The envelope function shows the distribution of the electron wave function (ψ_c) assuming the hole is fixed at the center of the coordinate system. Considering that ψ_c changes sign from the A to the B atom, the $n=1$ state is antisymmetric ($\sigma_n=-$) while $n=2$ is symmetric ($\sigma_n=+$). In the circumferential direction, the combinations of electrons and holes from around the K and K' points can be referred to as $K+K'$ and $K-K'$, whose parities are $\sigma_X=+$ and $\sigma_X=-$, respectively. Therefore, we obtain the following exciton states: $(n=1)\otimes(K+K')=1-$, $(n=1)\otimes(K-K')=1+$, $(n=2)\otimes(K+K')=2+$, $(n=2)\otimes(K-K')=2-$. Since the ground state is totally symmetric, for light polarized along the nanotube axis, one-photon absorption can only excite $\sigma_n=-$ exciton states, and two-photon absorption can only excite $\sigma_n=+$ exciton states. In both cases, $\sigma_X=+$ because the light polarization is along the nanotube axis. Such polarization cannot change the wave-function parity in the circumferential direction σ_X. Therefore, only 1− excitons are excited in one-photon experiments, whereas only 2+ excitons are excited in two-photon experiments. Although the E symmetry excitons are not allowed in either one-photon or two-photon optical transitions, they can play a role in the relaxation processes discussed in this work.

[14] F. Wang, G. Dukovic, L. E. Brus, and T. F. Heinz, Science **308**, 838 (2005).

[15] C. Thomsen and S. Reich, Phys. Rev. Lett. **85**, 5214 (2000).

[16] C. Rulliere, *Femtosecond Laser Pulses: Principles and Experiments* (Springer Sci.+Business Media, Inc., 2005).

[17] M. Zheng and B. A. Diner, J. Am. Chem. Soc. **126**, 15390 (2004).

[18] S. M. Bachilo, L. Balzano, J. E. Herrera, F. Pompeo, D. E. Resasco, and R. B. Weisman, J. Am. Chem. Soc. **125**, 11186 (2003).

[19] S. G. Chou, H. B. Ribeiro, E. Barros, A. P. Santos, D. Nezich,

Ge. G. Samsonidze, C. Fantini, M. A. Pimenta, A. Jorio, F. Plentz Filho, M. S. Dresselhaus, G. Dresselhaus, R. Saito, M. Zheng, G. B. Onoa, E. D. Semke, A. K. Swan, M. S. Ünlü, and B. B. Goldberg, Chem. Phys. Lett. **397**, 296 (2004).

[20] Since it is difficult to accurately resolve τ_{slow} within the initial decay of 20 ps, the pump fluence dependence for τ_{slow} shown in Fig. 2(b) was determined in a separate experiment with a longer scan time.

[21] R. B. Capaz (private communication).

[22] H. Zhao and S. Mazumdar, Phys. Rev. Lett. **93**, 157402 (2004).

[23] C. D. Spataru, S. Ismail-Beigi, R. B. Capaz, and S. Louie (unpublished).

[24] V. Perebeinos, J. Tersoff, and P. Avouris, Phys. Rev. Lett. **94**, 086802 (2005).

[25] F. Wang, G. Dukovic, E. Knoesel, L. E. Brus, and T. F. Heinz, Phys. Rev. B **70**, 241403(R) (2004).

[26] A. Hagen, M. Steiner, M. B. Raschke, Ch. Lienau, T. Hertel, H. Qian, A. J. Meixner, and A. Hartschuh (unpublished).

[27] M. Jones, C. Engtrakul, W. K. Metzger, R. J. Ellingson, A. J. Nozik, M. J. Heben, and G. Rumbles, Phys. Rev. B **71**, 115426 (2005).

[28] J.-P. Yang, M. M. Kappes, H. Hippler, and A.-N. Unterreiner, Phys. Chem. Chem. Phys. **7**, 512 (2005).

[29] J. S. Lauret, C. Voisin, G. Cassabois, P. Roussignol, C. Delalande, L. Capes, E. Valentin, and O. Jost, Semicond. Sci. Technol. **1**, S486 (2004).

[30] A. Maeda, S. Matsumoto, H. Kishida, T. Takenobu, Y. Iwasa, M. Shiraishi, M. Ata, and H. Okamoto, Phys. Rev. Lett. **94**, 047404 (2005).